

JGR Atmospheres

RESEARCH ARTICLE

10.1029/2019JD031647

Key Points:

- Mesoscale atmospheric motion vectors (AMVs) have been developed from rapid scan GOES-16 ABI measurements
- Assimilation of vortex-scale rapid scan AMVs in the HWRf model results in consistent track prediction improvements for Hurricanes Harvey, Irma, and Maria; improvements are mainly from better initialization of the wind fields in the vortex-scale region and near environment
- Through high spatiotemporal sampling of targeted tropical cyclones, the new generation of geostationary satellites provides important observational data for forecast improvement

Correspondence to:

J. Li,
jun.li@ssec.wisc.edu

Citation:





Li, J., Li, J., Velden, C., Wang, P., Schmit, T. J., & Sippel, J. (2020). Impact of rapid-scan-based dynamical information from GOES-16 on HWRf hurricane forecasts. *Journal of Geophysical Research: Atmospheres*, 125, e2019JD031647. <https://doi.org/10.1029/2019JD031647>

Received 11 SEP 2019

Accepted 22 JAN 2020

Accepted article online 27 JAN 2020

Impact of Rapid-Scan-Based Dynamical Information From GOES-16 on HWRf Hurricane Forecasts

Jinlong Li¹ , Jun Li¹ , Christopher Velden¹, Pei Wang¹ , Timothy J. Schmit² , and Jason Sippel³

¹Cooperative Institute for Meteorological Satellite Studies, University of Wisconsin-Madison, Madison, WI, USA, ²Center for Satellite Applications and Research, NOAA/NESDIS, Madison, WI, USA, ³NOAA Atlantic Oceanographic and Meteorological Laboratory, Miami, FL, USA

Abstract Observations of dynamical information in the upper levels of tropical cyclones at high spatiotemporal resolutions are rare but very important to the analysis and prediction of the storm evolution and landfall impacts. These observations are now becoming routinely available from the new generation of geostationary weather satellites. Understanding and optimizing the utilization of that information in numerical weather prediction models is a vital step toward simulating tropical cyclone behavior and improving forecasts. The Advanced Baseline Imager (ABI) onboard GOES-16 is providing high spatial and temporal resolution images that can be targeted on North Atlantic tropical cyclones. In addition to a full-disk scan every 10 min and a CONUS scan every 5 min, the ABI also has a flexible “mesoscale scan” mode featuring limited moving domains at 1-min intervals. The mesoscale scan can focus on a targeted storm center with a 10°×10° domain coverage that follows the storm movement. Using this 1-min ABI imagery to track cloud motions, automated algorithms have been developed to produce enhanced, high-resolution atmospheric motion vectors (AMVs) during a targeted tropical cyclone event. These high spatiotemporal AMVs represent estimates of the wind field around the storm and can provide critical dynamical information on the targeted storm and its near environment. This information can help improve the representation of the initialized vortex in numerical model analyses. To study the impact of the enhanced AMV observations on numerical weather prediction, the Hurricane Weather Research Forecast (HWRf) model is used in a series of assimilation and forecast experiments. Three destructive Atlantic hurricane cases from 2017, Harvey, Irma, and Maria, are chosen as case studies. The results show that the assimilation of the enhanced AMVs from GOES-16 consistently improves the HWRf hurricane track and size forecasts, and have mixed impacts on intensity forecasts. These results augment previously published studies on optimizing the quantitative use of new generation geostationary satellite rapid-scan observations for improving high impact weather forecasts.

1. Introduction

Reliable forecasts of major landfalling tropical cyclones (TCs) such as Hurricane Sandy (2012), Matthew (2016), Harvey (2017), Irma (2017), and Maria (2017) are critical for decision making and preparation. Obtaining good TC track and wind structure forecasts remains one of the most challenging aspects of high-impact weather prediction. Conventional observations of atmospheric water vapor (WV) variables and winds in the TC environment at high spatiotemporal resolution are rare but very important for accurate predictions of the storm evolution and landfall impacts. To help address this observational need, the Advanced Baseline Imager (ABI; Schmit et al., 2005, 2017, 2018) onboard National Oceanic and Atmospheric Administration (NOAA)'s new generation of geostationary weather satellites (GOES-R series, beginning with GOES-16 launched on 19 November 2016) is routinely providing high temporal (every 1 min) and spatial (0.5–2 km) resolution multispectral (16 bands) imagery that can target on TCs and quantify into rapid-update moisture variables and atmospheric motion vector (AMV) information.

Optimizing the utilization of that information in operational numerical weather prediction (NWP) systems such as the Hurricane Weather Research and Forecasting (HWRf) model is a vital step toward improving TC forecasts. Previous studies (Velden et al., 2017; Wu et al., 2014, 2015; Zhang et al., 2018) have shown that high-resolution AMVs can improve WRF/HWRf analyses and forecasts of TC structure and intensity. The

AMVs used in these studies were produced from the preceding generation of geostationary satellites (MTSAT and pre-GOES-R) in special scanning modes attempting to simulate the new generation (Himawari/GOES-R) rapid-scan data as close as possible at that time. The enhanced AMV data showed overall positive impacts from these studies even though different models, assimilation systems, and strategies were employed. Assimilation of layered precipitable water derived from the Advanced Himawari Imager onboard the Himawari-8 satellite also showed positive impact on TC forecasts (Lu et al., 2019; Wang et al., 2018). It is evident from these demonstrational studies that the high-resolution moisture and AMVs now available from the GOES-R series have the potential to provide beneficial forecast impact when assimilated into the operational HWRf model during Atlantic TC events.

The objective of this pilot study is to conduct HWRf assimilation experiments with newly available GOES-16 rapid-scan AMV datasets processed by the Cooperative Institute for Meteorological Satellite Studies (CIMSS) at the University of Wisconsin during three major Atlantic hurricanes in 2017. The experiments are performed on the NOAA/National Environmental Satellite, Data, and Information Service (NESDIS)-funded Supercomputer for Satellite Simulations and Data Assimilation Studies (S4; Boukabara et al., 2016), which is physically located at the University of Wisconsin-Madison's Space Science and Engineering Center (SSEC), using the NOAA Developmental Testbed Center (DTC) released HWRf v3.9a. The study focuses on the utilization and impact of the new GOES-16 high spatiotemporal resolution AMVs in the analysis-sensitive TC vortex region toward improving HWRf TC analyses and forecasts. The ABI rapid-scan mode and AMV data processing strategies are described in section 2. Section 3 gives a brief introduction to the HWRf model and assimilation system. Section 4 presents an overview of the selected hurricane cases, AMV data quality control (QC) procedures, and experiment design used in the study. In section 5, cumulative forecast impact results for the three hurricanes are shown, as well as individual case demonstrations. Finally, a summary of the findings is provided in section 6.

2. GOES-16 ABI Rapid-Scan Mode and Derived AMVs

2.1. ABI Rapid-Scan Mode

The “flex” image scan mode of the ABI offers two limited-area sectors every minute (Schmit et al., 2018). This means either 30-s image sampling if the center points are the same or as it is usually scheduled, 1-min imagery for two different locations. There are two such sectors from each ABI, hence a total of four from the GOES-East and West constellation. These sectors are 1,000 km by 1,000 km at the satellite subpoint, and all 16 available spectral bands of the ABI are provided in these scans. The data are available via a number of distribution means, including the real-time GOES-R reBroadcast and NOAA's CLASS archive. These scans are in addition to the contiguous U.S. and Full Disk (hemispheric) scans. To prepare for the operational rapid-scan imagery from the ABI, NOAA operated GOES-14 in an experimental mode over parts of 2012 to 2016, so that 1-min imagery could be obtained for both research and demonstration in operations (Schmit et al., 2014). Many phenomena were sensed, including, but not limited to convection, fog, hurricanes, and fires (Apke et al., 2016; Bedka et al., 2015; Lindley et al., 2016; Line et al., 2016; Mecikalski et al., 2015; Schmit et al., 2013). The ABI rapid-scan sectors have default coverage areas but are relocatable to any region within the full disk domain upon request from the National Weather Service. Specifically, TCs are often targeted, especially those with the prospects of making landfall. A recent example of GOES-16 ABI rapid-scan imagery for a period during Hurricane Dorian (2019) is presented in the CIMSS satellite blog (<https://cimss.ssec.wisc.edu/goes/blog/archives/34256>).

2.2. Vortex-Scale AMV Datasets

The upgraded sensor capabilities of the GOES-R Series can be exploited toward optimizing image product enhancements. For applications to TCs, high spatiotemporal wind observations are needed to resolve the smaller-scale flow fields. Crucial to obtaining these observations is the continuous 1-min image sampling over targeted storms as described above. In addition to using 1-min image triplets in the cloud tracking process, modifications to the strategies for deriving enhanced AMV (visible [VIS], infrared [IR], and WV) coverage (vs. routine full-disk processing) include increasing the target density, reducing the minimum gradient required for target identification, disabling stringent coherency requirements, and relaxing QC constraints

Table 1
GOES-16 ABI Spectral Channels Used to Derive the Different Types of AMVs

AMVs	Channel number	Wavelength	Spatial resolution
Visible	Channel 2	0.64 μm	0.5 km
IR shortwave	Channel 7	3.9 μm	2 km
IR water vapor	Channel 8	6.19 μm	2 km
IR longwave	Channel 14	11.21 μm	2 km

Abbreviations: ABI: Advanced Baseline Imager; AMVs: atmospheric motion vectors; IR: infrared.

(Stettner et al., 2019). All of these processing strategies are imposed to enhance AMV coverage and maximize the information content to resolve the scales of the flow fields associated with the TC vortex and its near environment.

For this study, the AMV datasets for three selected hurricanes in 2017 were processed using the strategies noted above by CIMSS from GOES-16 ABI rapid-scan imagery. The datasets were created at 15-min intervals for assimilation into the HWRF model. Four ABI bands were used to derive AMVs (Table 1): VIS (Channel 2), IR shortwave (Channel 7), IR WV cloud top (Channel 8), and IR longwave (Channel 14). The AMV derivation algorithm is basically the same as used for operational processing at

NOAA/NESDIS and employs a nested tracking technique (Bresky et al., 2012). To assign a height to a derived AMV for a cloud target, pixel-level cloud top pressures, outputted from a simultaneously executed cloud height algorithm, are processed. The median cloud top pressure in the target cloud is assigned as the representative height (Daniels et al., 2019). As mentioned above, the derived AMVs benefit from the improved temporal sampling of coherent cloud motions, and for this study the processing strategies have been optimized for the production of high-density vortex-scale AMVs (Stettner et al., 2019). It is expected that tailored GOES-16/17 mesosector AMV datasets will become operational at NOAA/NESDIS and be made publically available in real time in the near future.

3. Forecast Model and Data Assimilation System

The model and assimilation system used in the study is the NOAA DTC released HWRF system version 3.9a. HWRF is a NOAA operational hurricane model with coupled atmospheric and oceanic components. The atmospheric component uses the Non-hydrostatic Mesoscale Model (NMM) dynamic core of the WRF model (WRF-NMM), and the oceanic component uses the Princeton Ocean Model adapted for Tropical Cyclones (POM-TC). The physical processes in HWRF v3.9a include an updated Arakawa-Schubert cumulus parameterization (Han et al., 2017), Ferrier-Aligo cloud microphysics (Ferrier, 2005), the Rapid Radiative Transfer Model for General Circulation Models (RRTMG) for radiation calculations (Iacono et al., 2008), and the GFS Hybrid Eddy-diffusivity Mass flux scheme for the planetary boundary layer (Han et al., 2016).

The HWRF model is comprised of three nested domains with an outermost parent domain (d01) fixed in time and two nested inside domains (d02 and d03) following the predicted storm center movement. The horizontal resolutions of three domains are 18, 6, and 2 km; the corresponding domain sizes are $80^\circ \times 80^\circ$, $24^\circ \times 24^\circ$, and $7^\circ \times 7^\circ$, respectively. There are 75 vertical levels for each of the domains. The model top is set at 10 hPa. A more detailed description of HWRF v3.9a model can be found in the HWRF scientific documentation (Biswas et al., 2017).

The initialization of HWRF involves a few steps including interpolation, vortex initialization (VI), and data assimilation. The initial conditions for the parent domain (d01) are derived from the Global Forecast System (GFS) analysis, while the first guess for the two nested domains (d02 and d03) is a 6-hr forecast from the global data assimilation system (GDAS). After that, the vortex separation, relocation, and adjustment are applied in the VI process. The vortex can be taken either from a bogus profile, or a GDAS 6-hr forecast, or the previous HWRF 6-hr forecast depending on the forecast cycle, storm intensity, and previous HWRF forecast availability. During the adjustment, the vortex intensity, structure, and location are corrected based on the Tropical Cyclone Vitals data (Trahan & Sparling, 2012). Previous studies showed that the continuously cycled HWRF analysis could have large errors in both TC location and intensity without VI, which would degrade the HWRF forecasts (Lu et al., 2017; Zhang et al., 2018). Tong et al. (2018) also looked at the impact of vortex adjustments in 2016 HWRF forecasts and found that VI was still beneficial to the forecast, especially in setting the initial maximum wind speed.

The first guess fields with a corrected vortex in the two nested domains (d02 and d03) are further improved by using the HWRF Data Assimilation System (HDAS), which is based on the community Gridpoint Statistical Interpolation (GSI) system. The assimilation domains (called the ghost d02 and ghost d03) are larger than the forecast d02 and d03 and have corresponding domain sizes of $28^\circ \times 28^\circ$ and $15^\circ \times 15^\circ$, respectively. The enlarged assimilation domain can ingest more observational data for analysis improvement.

The full-capability HDAS mode is run with three-dimensional (3-D) hybrid ensemble variational data assimilation. The background error covariance is a combination of the static fields and the flow dependent fields from either the GFS ensemble forecasts or the HWRF ensemble forecasts. Due to computational resource limitations, only the static background error covariance was applied in this study. It should be noted that a blending process is employed in some situations after data assimilation. To avoid strong storm (maximum wind speed ≥ 65 kt) vortex spindown, the increments from the data assimilation analysis are removed below the 600-hPa pressure level if they are within 150 km of the storm center. The increments are gradually inserted between 150 and 300 km and fully implemented beyond 300 km.

To assure consistency in results from HWRF v3.9a on S4 and the operational HWRF, the life cycle of hurricane Irma (2017) was run on S4 with the settings described above. The S4 forecasts were compared with the operational HWRF forecasts, and the results were reasonably close. HWRF v3.9a does not have the capability to process GOES-16 ABI AMV data, so code to accomplish this was added to ingest GOES-16 AMV bufr data and perform QC processing. The tools have also been developed to convert AMV data into the bufr format that GSI uses. In this way, the rapid-scan AMVs from GOES-16 can be read and assimilated into the HDAS system. The QC procedures for the assimilated AMV data will be described in the next section.

4. Hurricane Cases, AMV Quality Control, and Experiment Design

4.1. Hurricane Cases

Three of the most destructive hurricanes in the Atlantic Ocean in 2017 were selected for this study. They are Hurricanes Harvey, Irma, and Maria. Two of them (Harvey and Maria) are the second and third costliest hurricanes in U.S. history, only behind Katrina (2005). Figure 1 shows the tracks of these hurricanes according to the National Hurricane Center (NHC) best track data set. After initially becoming a tropical storm on 17 August, Hurricane Harvey weakened to a tropical depression and further into a tropical wave at 18 UTC of 19 August. Harvey regenerated and began to intensify rapidly late on 23 August. It quickly became a hurricane on 24 August and reached a peak category 4 status before it made landfall on the coast of Texas. Harvey produced the most significant tropical rainfall event in U.S. history with more than 60 inches over southeastern Texas (Blake & Zelinsky, 2018).

Both Irma and Maria were category 5 hurricanes with corresponding peak maximum wind speeds of 155 and 150 kt, respectively (Cangialosi et al., 2018; Pasch et al., 2018). Hurricane Maria caused catastrophic damage in Dominica and Puerto Rico. With a landfall intensity of 145 kt, it was the strongest hurricane on record to make landfall in Dominica. Maria was of a similar intensity (135 kt) when it ravaged Puerto Rico. Hurricane Irma was one of the strongest long-lived hurricanes, lasting as a hurricane from 06 UTC, 31 August, to 06 UTC, 11 September 2017, and was at least category 3 strength for most of that period. Hurricane Irma made a total of seven island landfalls before it finally hit the southwestern Florida coast. It also caused widespread damage during its passage over the northern Caribbean Islands. Hurricane Maria experienced an extreme rapid intensification from 16 to 19 September with a maximum intensification rate of 70 kt per day. Hurricane Irma's intensification occurred over two periods, from 30 August to 1 September and from 4 to 5 September, with an average rate of increase in the maximum winds of about 36 kt per day.

In general, the NHC official track forecasts of these three hurricanes were pretty good, with the average errors being much lower than the mean official errors for the previous 5-year period for all forecast times, while the intensity forecasts were worse than the previous 5-year mean due to the strength of the storms. In comparison, the operational HWRF system forecasted the intensity pretty well statistically, being better than or close to the official forecasts most of the time, particularly for Hurricanes Irma and Maria. However, HWRF had some difficulties during rapid intensification periods (e.g., on 5 September for Hurricane Irma and on 18 September for Hurricane Maria in 2017). The operational HWRF track forecasts were generally ok but did have some notable deviations. For example, when Hurricane Irma was over the central-western Atlantic, it was predicted by HWRF to turn northward and make landfall over the southeastern United States similar to other models. But Irma actually moved mainly westward during that time and did not turn northward until much later, landfalling and impacting southwest Florida. For Hurricane Maria, the operational HWRF forecasts had a slight right of track bias before 06 UTC 19 September 2017. Though it is difficult to remove these kinds of forecast errors, better observations along with a good assimilation system could help reduce them.

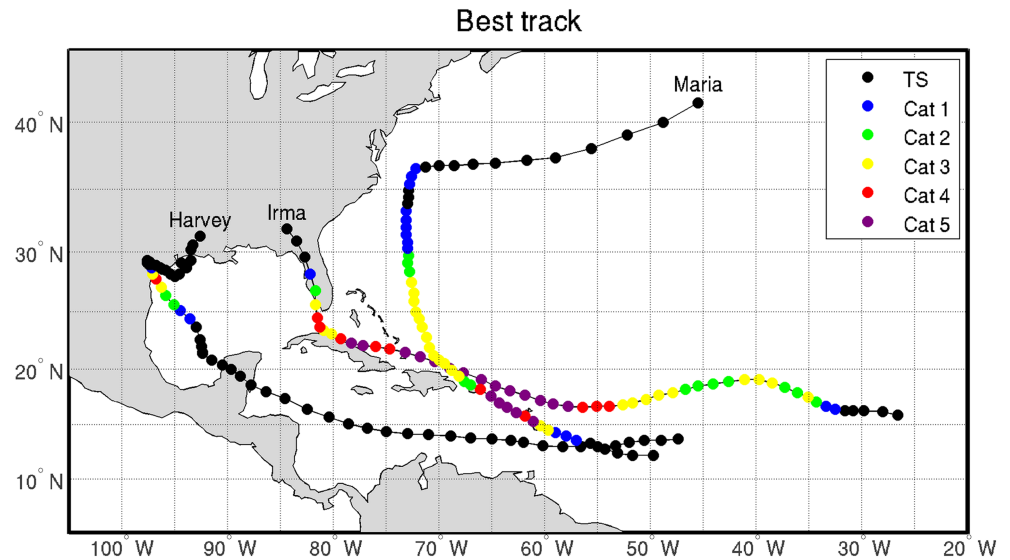


Figure 1. National Hurricane Center (NHC) best tracks for 2017 hurricanes Harvey, Irma, and Maria. Different colors on each track represent the intensity of the hurricanes on the Saffir-Simpson hurricane wind scale from category 1 to 5; the black indicates tropical storm (TS) strength.

4.2. AMV Data Quality Control

The GOES-16 rapid-scan AMV datasets for these three hurricane events were processed every 15 min, using a triplet of 1-min images for each time period to perform the cloud tracking. The data are spatially dense over the core of the hurricane and are bimodally distributed in the vertical. Most of AMVs are assigned pressure heights either above 350 hPa or below 650 hPa with corresponding peak levels at around 250 and 850 hPa, respectively. While the IR WV and IR longwave channels provide AMVs around the clock, the VIS channel only produces AMVs during daylight hours and the IR shortwave channel only during nighttime hours. Both

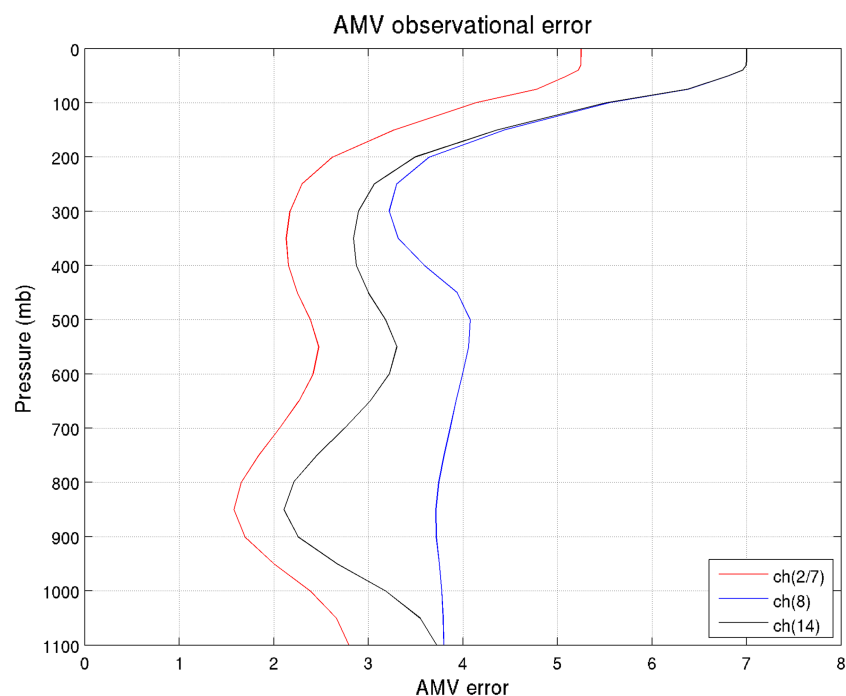


Figure 2. The vertical distributions of assigned atmospheric motion vector (AMV) observation error for each GOES-16 AMV type.

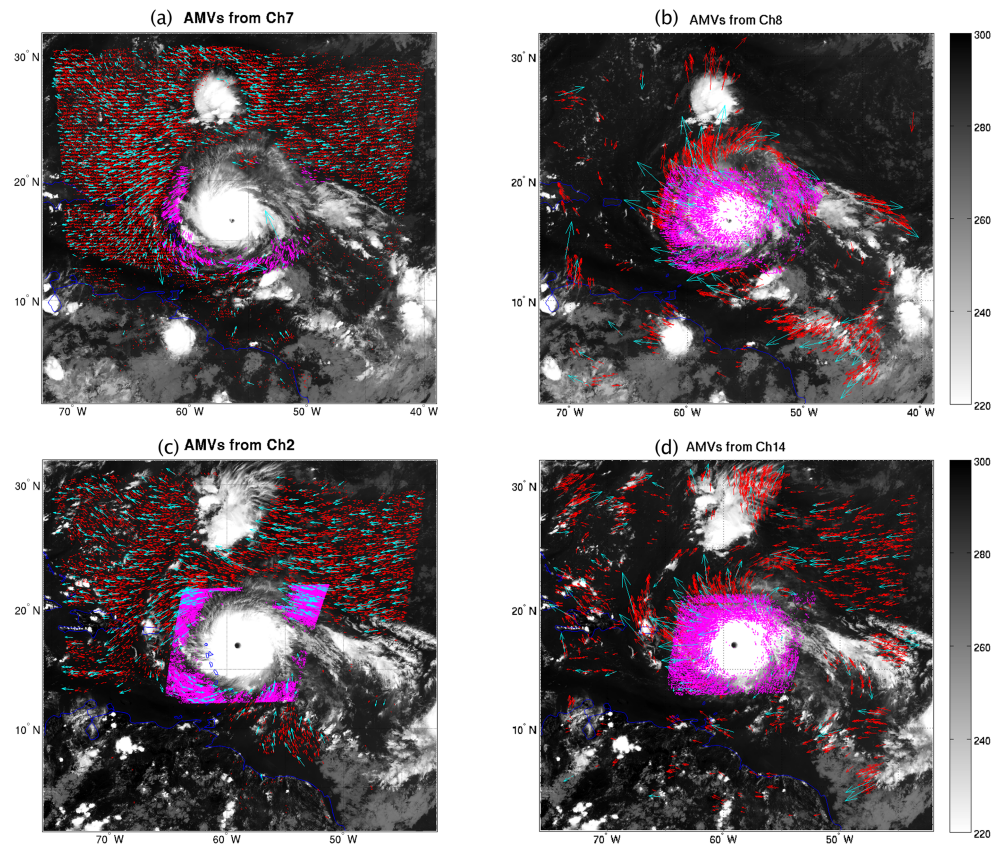


Figure 3. The data coverage from GOES-16 rapid-scan atmospheric motion vectors (AMVs; magenta) and operational GOES-13 AMVs (red) for (a) Channel 7 and (b) Channel 8 at 06 UTC, (c) Channel 2 and (d) Channel 14 at 18 UTC, 5 September 2017 during Hurricane Irma. By using the same AMVs from both GOES-16 and GOES-13, the wind vectors (cyan) are plotted over the top of original data, but at the reduced resolution. The GOES-16 IR Channel 14 provides the background imagery.

the VIS and SWIR are processed for low-level coverage only, while the LWIR channels provide AMVs at all heights. Most of the low-level AMV coverage is confined to the outer circulation of the hurricanes, away from the central dense overcast (CDO). Over the core region/CDO, the AMVs are mainly confined to tracking cirrus/outflow at very high levels. Some of these characteristics are demonstrated in Figures 3 and 4 in next section.

The AMVs also come with vector quality information based on a set of consistency and coherency tests that result in a quality indicator (QI, ranging from 0.1 [poor] to 1.0 [excellent]) for each vector. Based upon previous studies (Lim et al., 2019; Velden et al., 2017; Wu et al., 2014), the QI value threshold for acceptance was set to 0.8 so that only AMVs with QIs greater than 0.8 were passed to the next assimilation step.

The GSI has a general quality check before doing the assimilation, which removes any observations that differ significantly from the corresponding interpolated values in the background fields. The procedure is as the following:

$$(\text{observation} - \text{background}) > \text{gross} \times (\max(\text{errmin}, \min(\text{errmax}, \text{obserror})))$$

where gross is a constant for a specific observation type; errmin and errmax are the corresponding minimum and maximum errors; obserror is the observational error. The default observation error distributions are provided by the GSI system based on calibration/validation studies with GOES-16 proxy data. For this study we set the gross value as 2.5 for all GOES-16 AMV data and tightened the observation error distributions for channels 2 and 7 by a factor of 0.75 from the default. Figure 2 shows the observation error distributions for each AMV type in the study. After all of these steps, about 90% of the AMVs from VIS and IR shortwave channels and about 65% of the AMVs from IR WV and longwave channels are passed on for assimilation, on

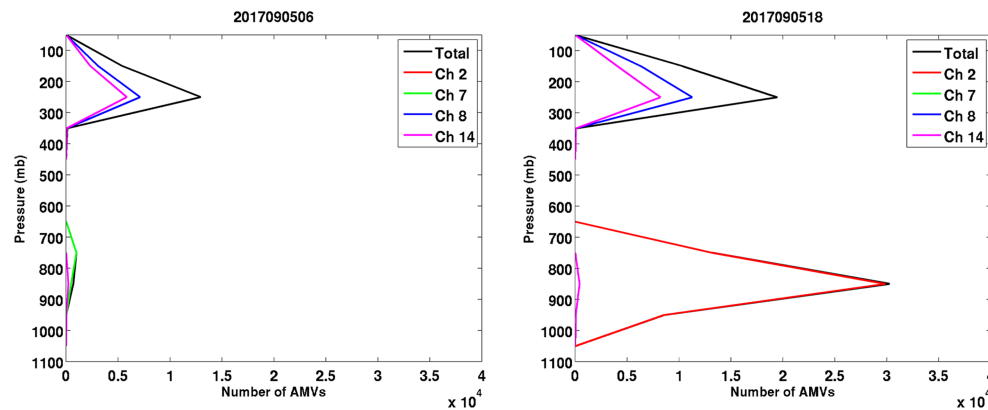


Figure 4. The vertical distribution of assimilated GOES-16 rapid-scan atmospheric motion vectors (AMVs) from the four channels at 06 UTC (left) and 18 UTC (right) on 5 September 2017.

average. Most of the discarded AMVs from the GSI QC step are upper-level vectors in the CDO region where the background fields are not adequately capturing the smaller-scale storm flow characteristics. This is a concern that will be addressed in future studies aimed at retaining this potentially important dynamical information over the core region that could affect the model intensity forecasts.

It should be noted that during the summer of 2107, the GOES-16 satellite was in its postlaunch test phase, and therefore, some image artifacts still existed (e.g., striping). However, it was deemed by the AMV derivation team that these effects were transient, and extra QC checks were applied before the assimilation stage to mitigate these effects.

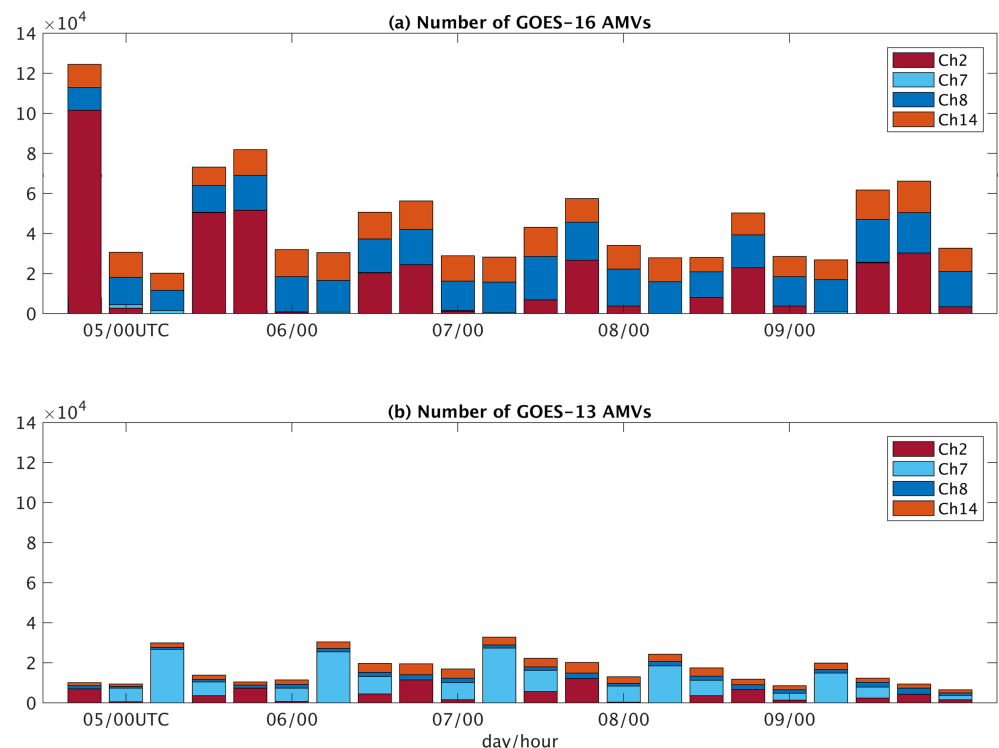


Figure 5. The number of assimilated (a) GOES-16 rapid-scan atmospheric motion vectors (AMVs) and (b) operational GOES-13 AMVs by channels during Hurricane Irma (2017) as a function of analysis time.

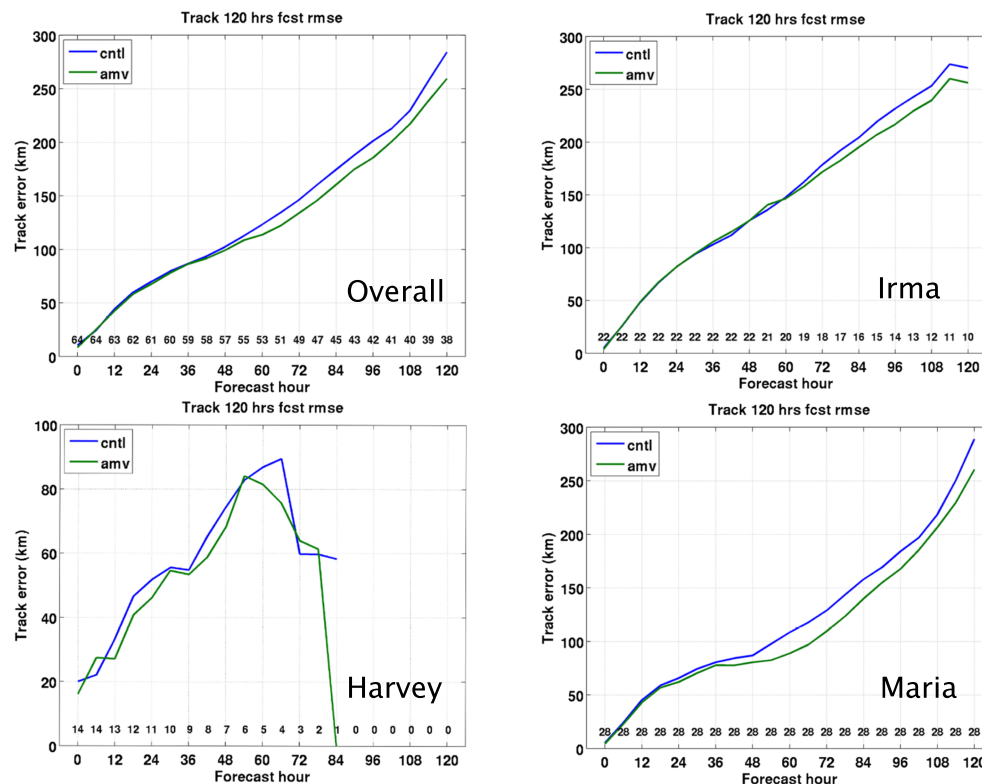


Figure 6. 120-hr Hurricane Weather Research Forecast (HRRF) track forecast root-mean-square error (RMSE) from the control (cntl, blue) and the GOES-16 rapid-scan atmospheric motion vector (amv, green) experiments for three hurricanes in 2017: Harvey, Irma, and Maria. An overall aggregate RMSE is also included. The numbers on the bottom of the plots are the cases used to compile the RMSE statistics. Note that the error scale for Harvey is much smaller than the other two storms due to the slow-moving nature of Harvey.

4.3. Experiment Design

To investigate the impacts of the GOES-16 rapid-scan AMVs on HRRF hurricane forecasts, two sets of experiments were run. In the control run, both conventional and satellite data from the National Centers for Environmental Prediction (NCEP) were used. Microwave radiances include data from the Advanced Microwave Sounding Unit (AMSU-A) onboard NOAA-15/18/19, Metop-A/B and NASA-Aqua, the Microwave Humidity Sounder (MHS) onboard NOAA-18/19 and Metop-A/B, and the Advanced Technology Microwave Sounder (ATMS) onboard Suomi-NPP. IR radiances include data from the High resolution Infrared Radiation Sounder (HIRS4) onboard NOAA-19 and Metop-A/B, Atmospheric Infrared Sounder (AIRS) onboard NASA-Aqua, the Infrared Atmospheric Sounding Interferometer (IASI) onboard Metop-A/B, and the Cross-track Infrared Sounder (CrIS) onboard Suomi-NPP. In addition, the operational satellite-derived AMVs from GOES-13 produced by NOAA/NESDIS at hourly intervals were also included. In the AMV experiment, the GOES-16 rapid-scan AMVs produced by UW/CIMSS were included in addition to all of the data used in the control run.

- CNTL: operational conventional and satellite data
- AMV: operational conventional and satellite data + GOES-16 rapid-scan AMV

Although the GOES-16 rapid-scan AMVs were available every 15 min, the HDAS only provides assimilation cycles in 6-hr intervals. Within each 6-hr time window, a method called First Guess at Appropriate Time (FGAT) was used so that the innovations (observation minus background) could be calculated at the observation time. This procedure used the GDAS forecast and previous HRRF forecast valid at the analysis time as well as three hours before and after the analysis time to create a time interpolation of the background for each observation. In this way the background at any time within the analysis time window could be interpolated and compared with observations. The calculated increments from this strategy are more realistic in representing the observation information content.

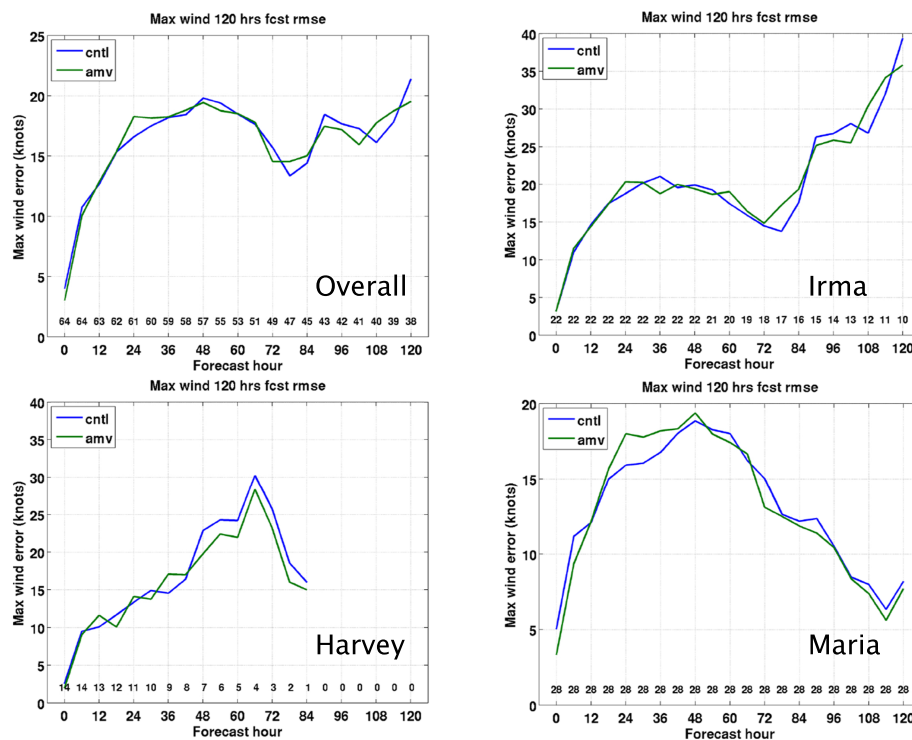


Figure 7. 120-hr Hurricane Weather Research Forecast (HWRF) maximum wind speed forecast errors (root-mean-square error [RMSE], kts) from the control (cntl, blue) and the GOES-16 rapid-scan atmospheric motion vector (amv, green) experiments for three hurricanes in 2017: Harvey, Irma, and Maria. An overall aggregate RMSE is also included. The numbers on the bottom of the plots are the cases used to compile the RMSE statistics.

Following each cycled analysis, a 120-hr forecast is produced. Based on the availability of GOES-16 AMV data, HWRF experiments are conducted for the Hurricane Harvey case from 06 UTC, 23 August, to 12 UTC, 26 August 2017; for Hurricane Irma from 18 UTC, 4 September to 00 UTC, 10 September 2017, and for Hurricane Maria from 00 UTC, 17 September to 18 UTC, 23 September 2017. A total of 64 analyses and forecasts are produced to assess the impact of the GOES-16 rapid-scan AMVs.

5. Results and Impact Analysis

5.1. Distribution of AMVs

The typical horizontal distribution of the specially processed GOES-16 AMVs after the assimilation steps are shown in Figure 3 as an example. The specially processed GOES-16 rapid-scan AMVs after QC (magenta vectors), superimposed on operational GOES-13 AMVs (red vectors) at 06 UTC (upper row) and 18 UTC (lower row) on 5 September 2017 are derived from channels 2 (VIS), 7 (SWIR), 8 (WV), and 14 (LWIR). Hurricane Irma is centered near 16.6°N, 56.4°W, and 16.9°N, 59.2°W, at these two corresponding times. The channel 2 data (VIS) are missing during the night (06 UTC), and the channel 7 data (shortwave IR) are not available around local noon time (18 UTC) due to solar reflection. It can be seen that there are many more AMVs from GOES-16 rapid-scan observations in the vicinity of the storm. These vortex-scale AMVs provide more dynamical information within the storm's cloud canopy and near environment, where the operational product is lacking. It should be noted that there appears to be limited AMVs over the TC inner core, even with this enhanced version of the processing. This is mostly due to the QC procedures in the HWRF assimilation process and could be important to the VI process and intensity forecasts discussed later. Future work will investigate better QC/assimilation strategies in order to maintain the AMV information over the storm core region.

The corresponding vertical distributions of GOES-16 AMVs are presented in Figure 4 and basically show a bimodal distribution with one peak around 250 mb and another between 750 and 850 mb. WV (ch. 8) and

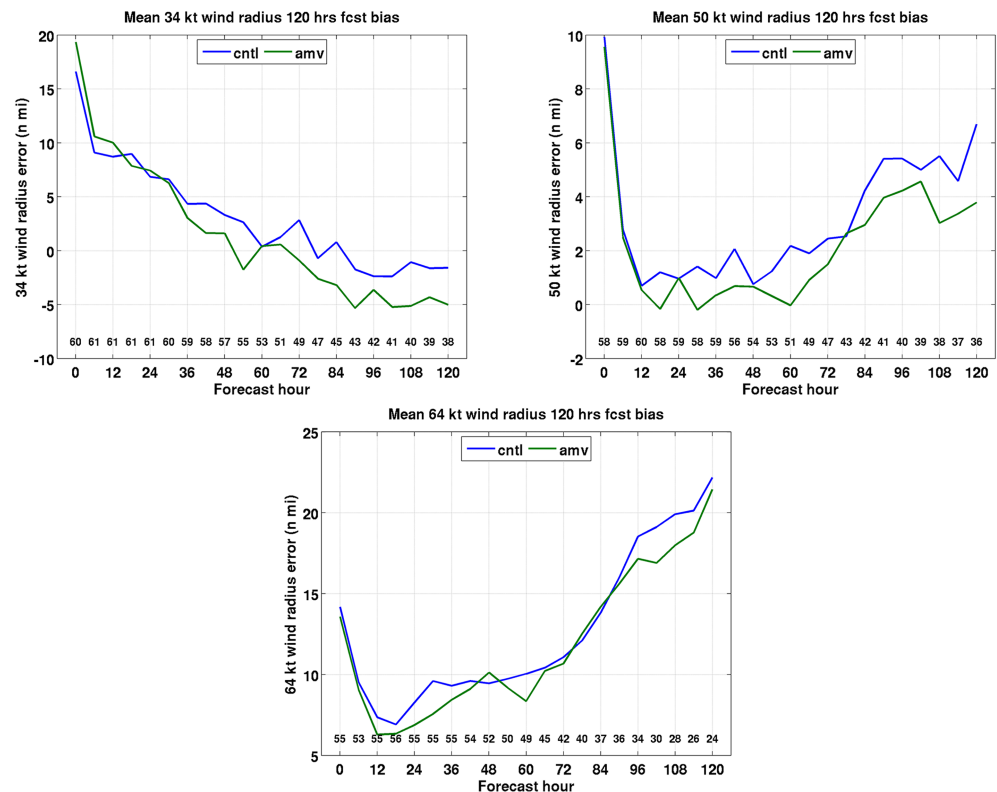


Figure 8. Overall Hurricane Weather Research Forecast (HWRF) hurricane size (surface wind radii) forecast errors from the control (cntl, blue) and the GOES-16 rapid-scan atmospheric motion vector (amv, green) experiments for the aggregate three hurricanes in 2017: Harvey, Irma and Maria. (upper left) 34 kt radius, (upper right) 50 kt radius, and (lower middle) 64 kt radius. The numbers on the bottom of the plots are the cases used to compile the error statistics.

longwave IR (ch. 14) AMVs dominate above 400 mb, while the VIS (ch. 2) and shortwave IR (ch. 7) AMVs dominate below 600 mb.

Figure 5 shows the number of GOES-16 AMVs (upper panel) and the operational GOES-13 AMVs (lower panel) assimilated into the GSI system as a function of analysis time for Hurricane Irma (2017). In general, 38% of the total assimilated GOES-16 AMVs are from the VIS band, 35% are from the WV cloud-top band, 26% are from the IR longwave band, and only 1% are from the IR shortwave band. The number of operational AMVs (GOES-13) is much less than the GOES-16 rapid-scan AMVs for most of the cycles, even though the operational AMVs cover a much larger domain. This is because the operational AMV processing is not optimized/enhanced for TC coverage and is instead focused on larger-scale coverage. As a result, there is quite a contrast in the operational AMV channel distribution, with about 51% of the total operational AMVs coming from the IR shortwave band (channel 7), and the number of AMVs from the rest three channels (channels 2, 8, 14) are about 20%, 11%, and 18%, respectively. The operational GOES-13 AMVs are distributed more in the low levels, while the GOES-16 rapid-scan AMV datasets provide a much larger share in the upper troposphere due to the extent of higher clouds from the TC covering much of the meso sector domain. Similar data distributions and behavior are found for other two TC cases.

5.2. HWRF Forecast Impact Results

Figure 6 shows the HWRF hurricane track forecast performance in terms of root-mean-square errors (RMSEs) for the three selected hurricane cases, and the aggregate. Best Track data from the NHC are used as the verifying tracks. By assimilating the GOES-16 rapid scan AMVs in addition to the routine operational data, the overall impact (upper left) on the hurricane track forecasts consistently improves after about 54 hr (about 8% after 60 hr). Considering the individual storms, Hurricane Maria shows the biggest track forecast improvement with an average RMSE reduction of about 10%. Hurricane Irma's impact mainly becomes

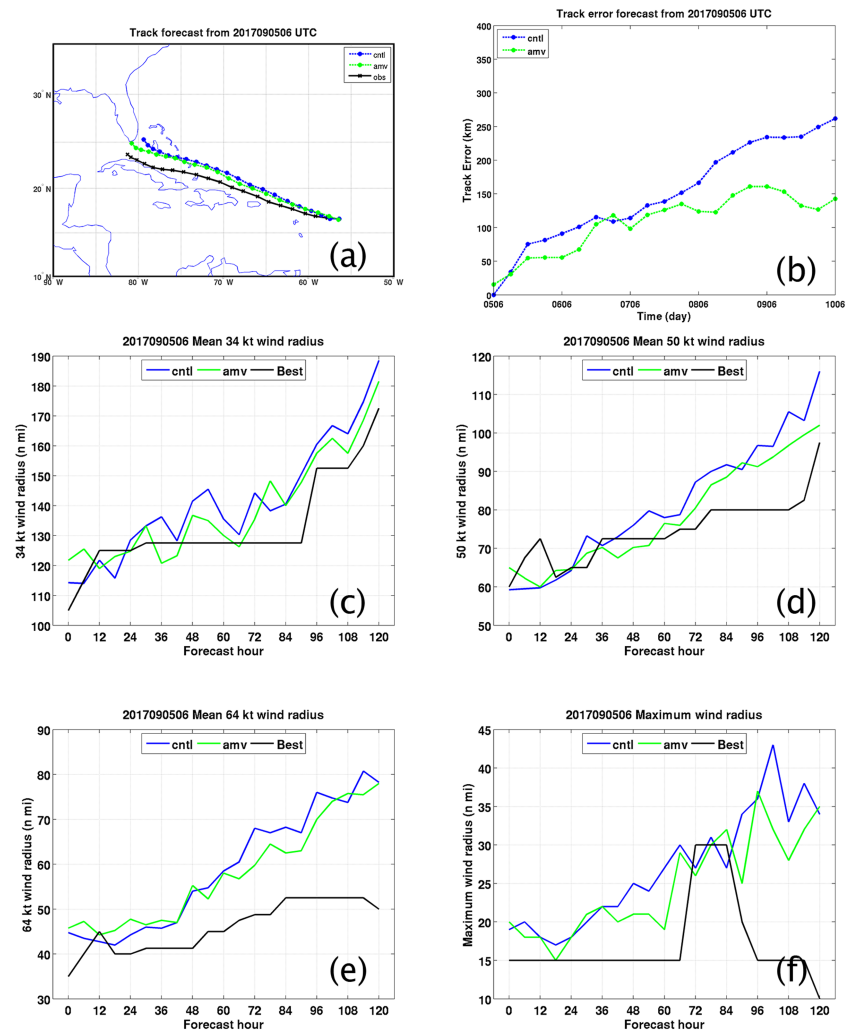


Figure 9. The 120-hour Hurricane Weather Research Forecast (HWRF) forecasts for Hurricane Irma initialized at 06 UTC 5 September 2017. (a) Track, (b) track error (km), (c) 34 kt wind radius (n mi), (d) 50 kt wind radius (n mi), (e) 64 kt wind radius (n mi), and (f) maximum wind radius (n mi). The black line is the Best Track data, blue for the control run, and green for the GOES-16 rapid-scan atmospheric motion vector run.

evident after about 60 hr, and Hurricane Harvey shows a small but consistent positive impact over a shorter forecast interval and limited cases.

The HWRF hurricane intensity (maximum wind speed) forecast RMSEs are given in Figure 7. Unlike the reduction in track forecast errors, the impacts of the GOES-16 rapid scan AMVs on HWRF maximum wind speed forecasts are somewhat mixed (minimum central sea level pressure forecasts show similar results, not shown). These results are perhaps not too surprising for several possible reasons. First, much of the inner core AMV information is lost in the QC process as discussed in sections 4 and 5.1. Retaining this information in the assimilation stages is likely crucial in establishing the upper level divergence profile at the top of the storm vortex, which will impact the vertical motion profiles and intensity. This aspect is being investigated further. Secondly, during the HWRF VI process, pseudo observations are inserted from the “TC Vitals” records provided by NHC, constraining the vortex strength and size and therefore limiting the inner core influence of the AMV data. Finally, the use of a static covariance in the assimilation process could hinder the information content of the rapidly updating AMVs in helping to define the vortex-scale flow fields. Ensemble approaches may provide some help in this regard. In summary, an improved treatment of the hurricane vortex region in the model QC, assimilation and initialization processes should allow a better chance for the AMV information to impact the intensity forecasts.

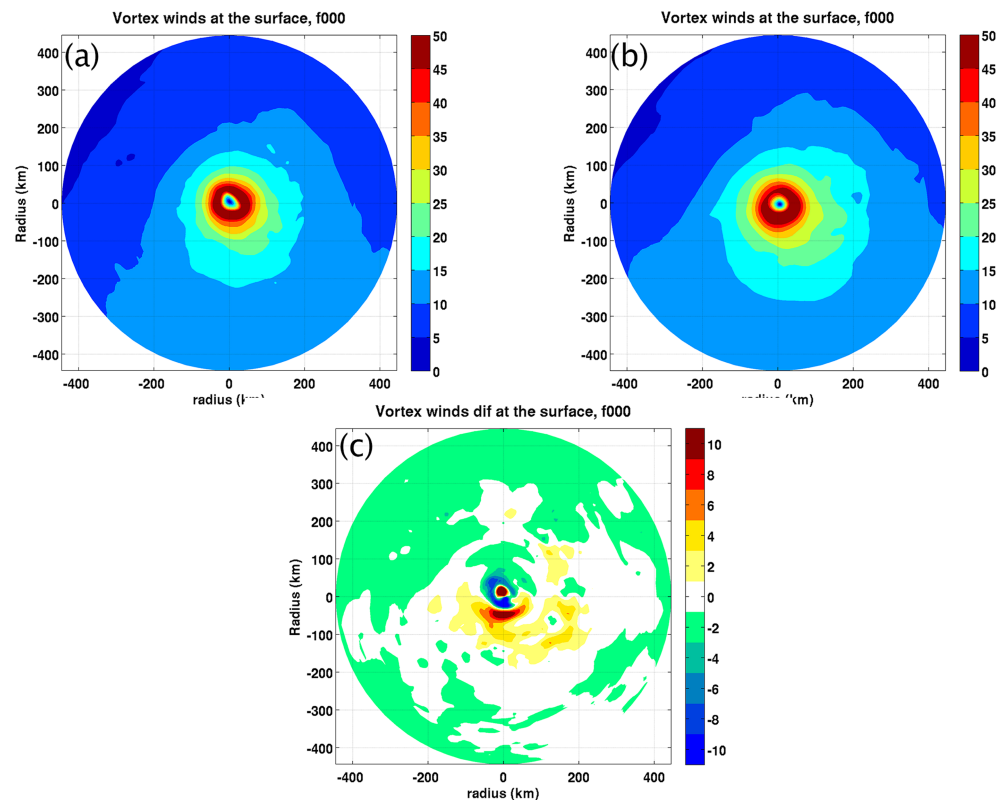


Figure 10. Hurricane Weather Research Forecast (HWRF) vortex wind speed at the surface for Hurricane Irma from the analysis time at 06 UTC on 05 September 2017. (a) CNTL run, (b) atmospheric motion vector (AMV) exp., (c) AMV-CNTL. (unit: m/s).

In addition to the track and intensity, storm size is another important forecast parameter. Figure 8 shows the HWRF forecast biases for hurricane size (expressed as surface wind radii) for the 34 kt wind radius (R34), the 50 kt wind radius (R50) and the 64 kt wind radius (R64) respectively. To calculate the mean bias for each wind radius size (R34, R50, R64), the radii over four different quadrants are averaged (if they all exist). As with the track and intensity, the observed wind radius data are obtained from the Best Track data provided by the NHC.

Figure 8 shows that there is a clear bias in storm size at the initialization time (the vortex is too large), and this carries forward through most of the wind radii forecasts. After an adjustment period during the first 12 hr or so, the biases for R50 and R64 steadily increase with forecast time. For R34, the biases are positive before 48 hr and then gradually become negative, especially for the AMV experiment. Comparing the two sets of experiments, the AMV run generally exhibits smaller biases at almost all times for R50 and R64. The AMV experiment also creates a smaller storm at larger surface wind radii (R34) after about 30 hr. These results demonstrate that the GOES-16 rapid-scan AMVs act to reduce the storm size bias in the HWRF forecasts.

5.3. Impact Analysis and Understanding

The assimilation of AMVs directly affects the wind structures and then further adjusts the temperature and moisture fields through the background error covariance matrix. The subtle modifications of the analysis fields can grow large enough to substantially change the forecast fields through the nonlinear interactions in the model. Figure 9 shows the HWRF track and track errors in a 120-hr forecast of Hurricane Irma initialized at 0600 UTC 5 September 2017. Starting from the analysis, the forecasted storm in the CNTL run moves northwest of and behind the Best Track, while the AMV run moves Irma a little faster and closer to the Best Track (Figure 9a). The track errors (Figure 9b) demonstrate more improvement for the longer

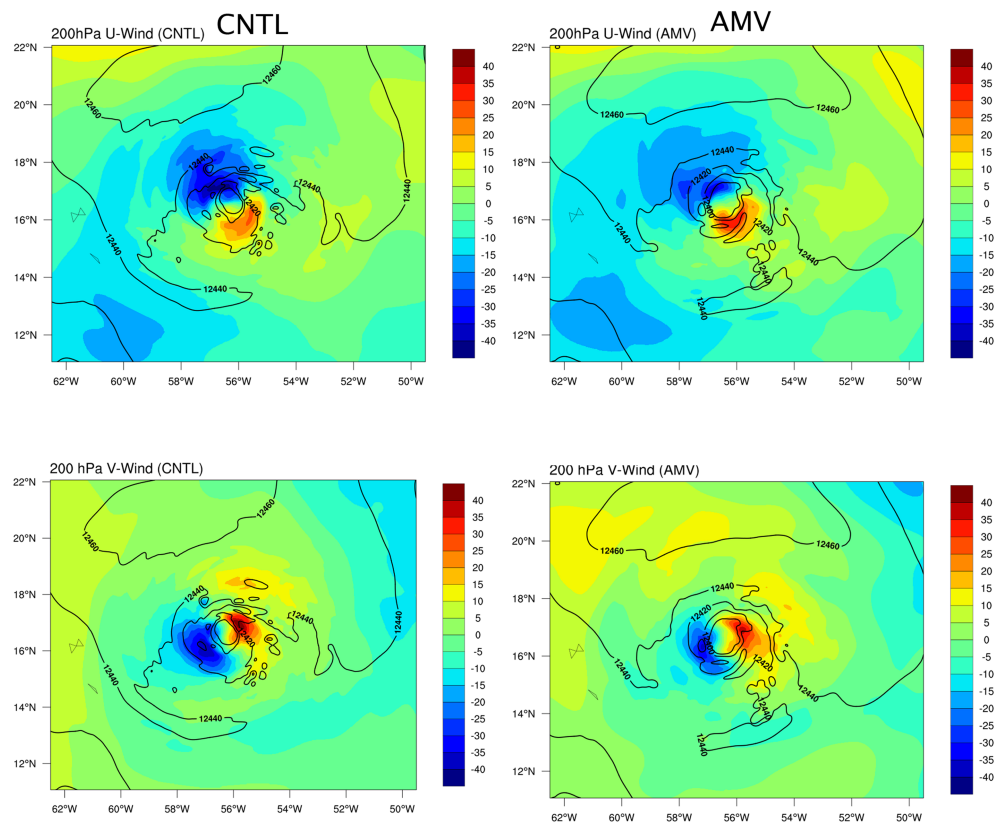


Figure 11. Hurricane Weather Research Forecast (HWRF) analysis increments of (u , v) at 200 hPa (colored unit: m/s) for the CNTL (left), and the atmospheric motion vector (AMV; right) experiments for Hurricane Irma at 0600 UTC 5 September 2017. The geopotential height (m) is also contoured.

forecast times. Figures 9c–9f show the corresponding HWRF hurricane size forecasts for the R34, R50, R64, and the radius of maximum wind. The hurricane size increases with time in both the Best Track and HWRF forecasts during the period. After 36 hr, the hurricane size in the AMV experiment is smaller and closer to the Best Track at all wind radii. Compared with the CNTL, the more realistic size of the hurricane in the AMV experiment could be contributing to the improved the hurricane track forecasts noted earlier.

To better view how the HWRF TC wind structure varies due to assimilating the GOES-16 rapid-scan AMVs, the surface vortex wind speed at the same analysis time is plotted in Figure 10 for both experiments. Within 100 km of the storm center, there is a more asymmetric appearance in the control run, with the shape of the vortex being stretched out along a northwest to southeast direction, especially near the storm center. Meanwhile, the AMV run shows a more symmetric structure to the vortex wind field. In the inner core, the surface wind analyses reveal a stronger storm with a larger eye in the CNTL. Farther from the storm center, the wind field is more expansive in the AMV run at the analysis time, consistent with Figure 9.

The corresponding analysis increments of (u , v) components at 200 hPa are shown in Figure 11. Comparing the two experiments, both have similar (u , v) dipole structures and indicate divergence at 200 hPa. Looking at the increment magnitudes, the AMV run values are slightly lower near the storm center, consistent with a weaker storm intensity as indicated by the vortex eyewall wind differences in Figure 10c.

Figure 12 shows the HWRF forecasted vertical cross sections of mean tangential wind of Hurricane Irma starting from the same analysis time (06 UTC 5 September, 2017). To calculate mean tangential wind, the model latitude-longitude grids are first converted into cylindrical coordinates centered on the storm, and then the regular wind components (u , v) are converted into tangential and radial components. The mean tangential winds are finally computed by averaging the tangential winds along the azimuth angles around the storm center. The solid bold black lines represent the radius of maximum tangential wind (RMTW). At the

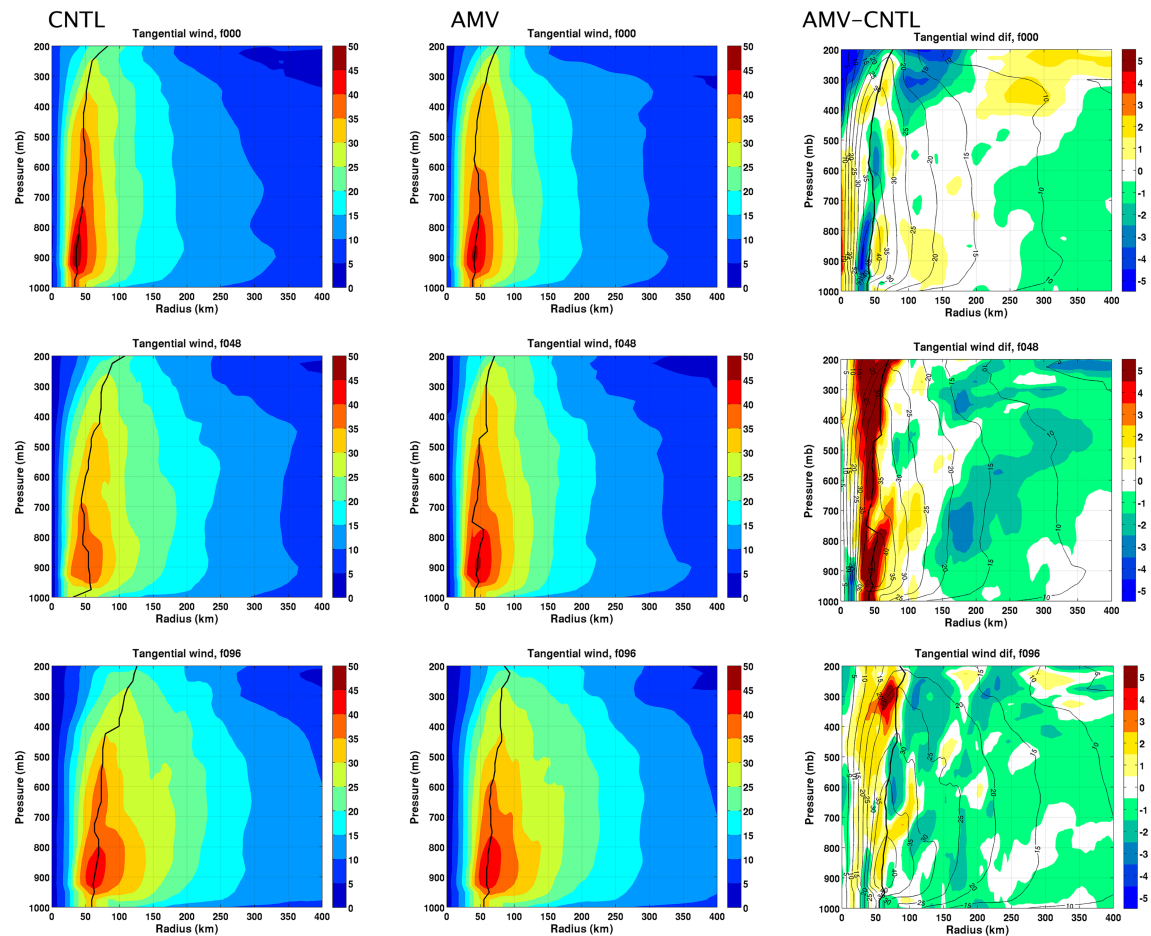


Figure 12. Hurricane Weather Research Forecast (HWRF) vertical cross sections of mean tangential wind (m/s) for Hurricane Irma at forecast times of (top) 00, (middle) 48, and (bottom) 96 hr. (left) CNTL run; (middle) atmospheric motion vector (AMV) exp.; (right) AMV-CNTL. The forecast starts from 06 UTC 5 September 2017. The solid bold black lines are the radius of maximum tangential wind (RMTW). The contour and bold lines in the right column are the same plots for the AMV run as in the middle.

analysis time, both experiments have similar tangential wind distributions with a maximum at around 900 hPa. Comparing the two, the magnitudes and the horizontal gradients of wind around the RMTW are larger in the CNTL run. The difference between the AMV and the CNTL runs shows that most of the vortex region within a 250-km radius and below 400 hPa indicates stronger tangential winds with the AMV analysis, except the area close to the RMTW. The negative values around the RMTW and the positive values inside the RMTW imply a stronger storm in the CNTL run, while the positive values outside the RMTW represent stronger winds, inferring a larger storm size in the AMV run. Along with the larger RMTW, these are consistent with the results shown in Figure 9, which demonstrate the storm sizes at all wind radii are larger on the surface with assimilating the GOES-16 AMVs at the initial time.

At 48 hr into the forecast, the CNTL storm weakens and its size increases at all levels. The signs of the differences below 850 hPa inside the RMTA are completely opposite to that of the initial time, now showing a stronger storm in the AMV run. The storm sizes increase for both the CNTL and the AMV experiments, more so with the CNTL run. In general, adding the GOES-16 rapid-scan AMVs in this case results in a smaller forecasted storm size not only near the surface but in the most of troposphere. The more expansive wind field in the CNTL run might be responsible for its northward forecast track bias through an increased beta effect (also called beta drift).

Another example is shown for Hurricane Maria at 18 UTC 18 September 2017 (Figure 13). Similar to the Irma case, the HWRF CNTL track forecast is generally too far north and east with respect to the Best Track. In the first 36 hr of the HWRF forecast, the CNTL and AMV storm tracks are very close. After that time, the AMV

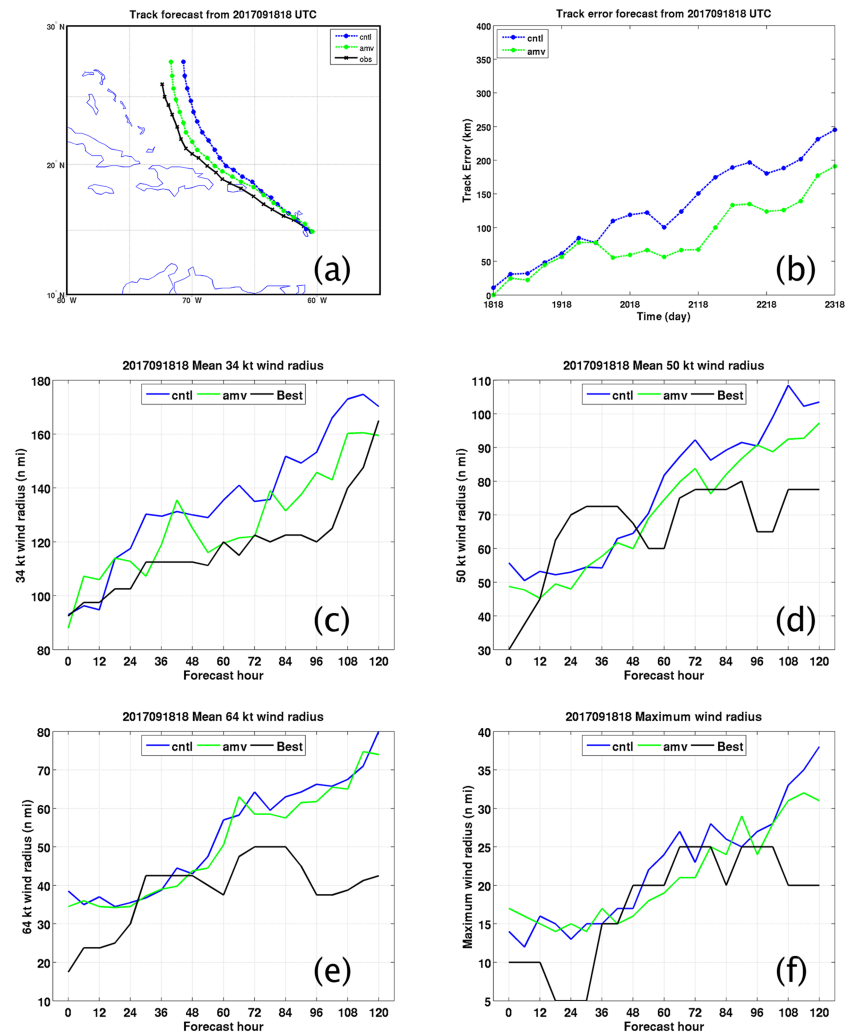


Figure 13. The 120-hour Hurricane Weather Research Forecast (HWRf) forecasts for Hurricane Maria initialized at 18 UTC 18 September 2017. (a) track, (b) track error (km), (c) 34 kt wind radius (n mi), (d) 50 kt wind radius (n mi), (e) 64 kt wind radius (n mi), (f) maximum wind radius (n mi). Black line is the Best Track data, blue for the control run, and green for the GOES-16 rapid-scan atmospheric motion vector run.

experiment track is farther west and closer to the Best Track. Figure 13b shows a clear split in the track error plot with errors at 96 hr about 124 and 180 km, respectively, for the AMV and the CNTL runs. With regard to forecast storm size, the R34 and R50 show a more consistent larger size reduction in the AMV experiment. R64 and radius of maximum wind also have a size reduction at most of forecast times, but smaller and less consistent.

Figure 14 shows the HWRf forecasted wind structures at three different wind speed ranges (>34 , >50 , and >64 kt) and four different pressure levels (250, 500, 750, and 1,000 hPa) for the same Maria case. At the analysis time (0-hr forecast at the top), both the CNTL and the AMV runs have similar storm centers close to the observed location. The wind fields in the CNTL are more symmetric at low levels (750 and 1,000 hPa) than in the AMV experiment, which is elongated along the east-west direction, particularly for >34 -kt winds. At 250 hPa the AMV run has a region of strong wind speed >64 kt on the southeast side of the center, while the CNTL depiction of >64 kt is broken into two parts around the center. After 48 hr into the forecast, the storm strengthens and widens in both experiments. The wind field shape and intensity are also similar. By 96 hr, the storm in the CNTL run at lower levels is larger and the shape more elongated in the northwestern to south-eastern direction than in the AMV experiment. The mean tangential wind distribution (not shown) indicates

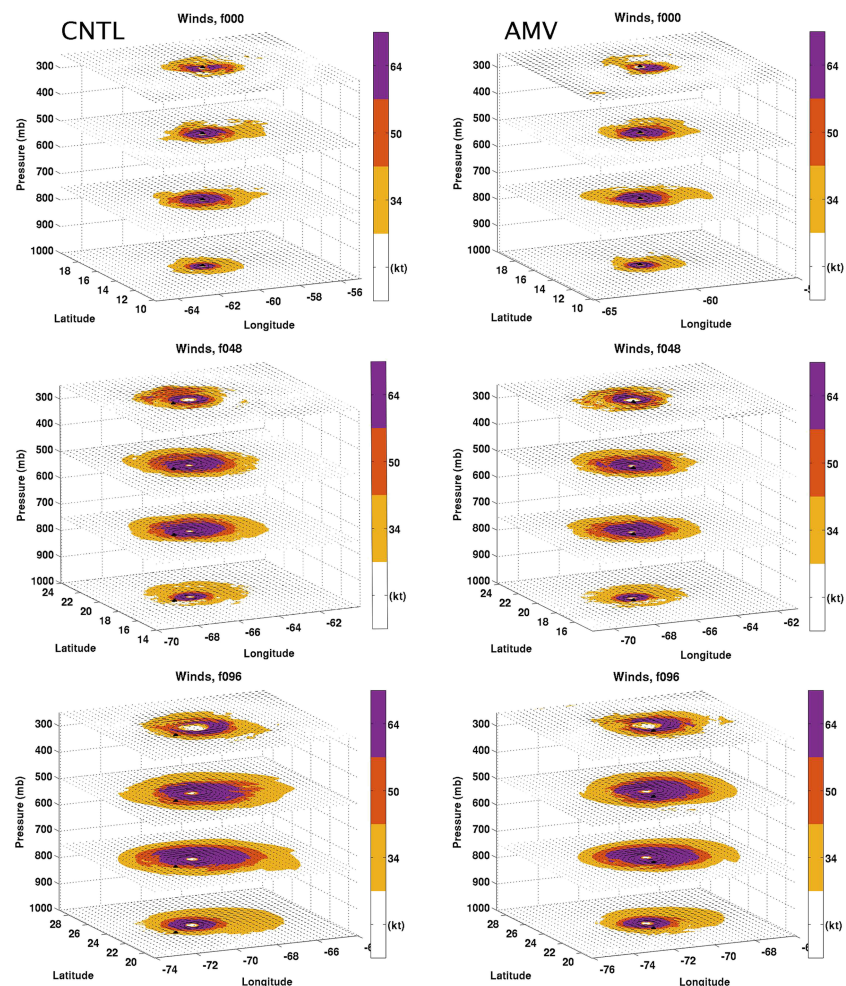


Figure 14. Hurricane Weather Research Forecast (HWRF) wind structure forecasts from Hurricane Maria for four pressure levels (250, 500, 750, and 1,000 hPa) starting from 18 UTC 18 September 2017. Left column: cntl run, right column: AMV exp. Top row: 0 hr forecast, middle row: 48 hr forecast, bottom row: 96 hr forecast. The three colors represent the 3 different wind speed ranges: purple for >64-kt wind, orange for >50-kt wind, and yellow for >34-kt winds. The observed hurricane center location at each forecast time is marked by the black point.

a stronger tangential wind in the CNTL from the beginning to the end of the forecast. Therefore, the track forecast differences between the CNTL and the AMV runs for Hurricane Maria could again result from the different beta effects also noted in the Irma case.

6. Summary

Enhanced, hurricane-scale AMVs derived from tracking cloud motions in rapid scans provided by the new generation of geostationary weather satellites are becoming increasingly available. These AMVs can depict the smaller-scale flow fields associated with TCs as they interact with their near-environment, impacting analyses and NWP forecasts after assimilation. This novel source of dynamic information is only available from new imaging sensors with a rapid-scan mode (e.g., images produced every 1–2.5 min) and flexible targeting capabilities (over a limited-area domain such as a moving TC). The enhanced AMV datasets examined in this study were obtained from 1-min image scans from the ABI on board GOES-16. During the processing of the images into AMV fields, special strategies have been applied to enhance the AMV coverage and maximize the information content on the scale of a hurricane. As a demonstration of the potential impact of these data on TC forecasts, high spatiotemporal AMV datasets were processed for three significant Atlantic hurricanes that occurred in 2017. The data were then assimilated into the HWRF hurricane model to assess forecast impacts.

In the assimilation of these high-resolution AMV datasets prior to the model initialization, modified QC steps were invoked in order to retain the added wind information content over the storm core and near environment. Here we used a combination of vector quality information provided during the AMV processing (vector Quality Indicator, QI) and an adjustment to the normal observation error profiles for AMV data types. Only AMVs with a QI greater than 0.8 were used in the assimilation, based on previous studies. The traditional observation error profiles of AMVs and associated QC settings are mainly based on the global model systems and operational AMV observations. These settings and profiles are not optimized to retain smaller-scale flow features. After limited empirical experimentation, looser constraints in the GSI gross error check and adjusted observation error profiles for channels 2 and 7 (VIS and shortwave IR) by a factor of 0.75 were adapted. Despite these modifications, a large percentage of the AMVs over the storm core region were not provided to the assimilation step, warranting further attention in future experiments

After applying these QC procedures, the GOES-16 rapid-scan AMVs were assimilated into HWRF in addition to conventional data, satellite radiances, and operational GOES-13 AMVs. The results versus control runs without the enhanced GOES-16 AMVs for three selected hurricanes in 2017 (Harvey, Irma, and Maria) demonstrate a consistent forecast track improvement, with also a notable reduction in the storm size bias especially at longer forecast lead times. Intensity forecasts yield mixed results, as impacts are generally small.

It should be noted that only a 3DVAR version of HDAS was used in this study due to limited computer resources. 3DVAR uses a static background error covariance matrix, which is mainly constrained by large-scale geostrophic balance. Lu et al. (2017) pointed out that using a static background error covariance might not be optimal for the TC inner-core data assimilation, and using a flow-dependent error covariance from self-cycled ensemble forecasts could achieve better dynamic and thermodynamic coherency for the TC vortex structure. With that in mind, it is expected that the rapid-scan AMVs could provide further positive forecast impacts (especially for TC intensity) by using the HDAS hybrid-ensemble assimilation method along with improved GSI QC optimization. Advanced assimilation could further show finer inner vortex structure changes, which are hardly demonstrable in this study. Finally, the frequent temporal sampling of the AMV datasets could be explored with the more frequent assimilation cycles. A 6-hr cycle was used in this study, but a shorter cycle interval (e.g., 3 hr or even 1 hr) could better match the observation times, which would be helpful in fast-changing vortex region conditions.

While the initial results presented in this study are promising, it is likely that the full information content of the enhanced AMV datasets in the TC core region is not entirely being realized. To address this, future work will focus on optimizing the AMV and GSI QC procedures, examining ensemble-based background error covariances, and including more frequent assimilation cycles. The balance of AMV data assimilation and VI may also need more attention to get the most benefit from the TC inner core AMV data.

Acknowledgments

This work was supported by the NOAA GOES-R Risk Reduction program (NA15NES4320001). Thanks to the UW/CIMSS satellite winds team for providing the GOES-16 ABI rapid-scan AMV data, and the JCSDA for providing the “S4” supercomputer resource located at UW/SSEC. The authors would also like to thank two reviewers for their many valuable comments to help us improve the quality of this paper. The GFS/GDAS analysis/forecast data, conventional observations, and satellite radiances can be obtained or requested from <https://ftp.ncep.noaa.gov/data/ncdf/com/gfs/prod/or> <https://www.ncdc.noaa.gov/>. The hurricane best track files were obtained from the National Hurricane Center <https://www.nhc.noaa.gov/data/>. GOES-16 ABI data are available from NOAA CLASS <http://www.class.noaa.gov>. The view, opinions, and findings contained in this report are those of the authors and should not be construed as an official National Oceanic and Atmospheric Administration's or U.S. government's position, policy, or decision.

References

- Apke, J. M., Mecikalski, J. R., & Jewett, C. P. (2016). Analysis of mesoscale atmospheric flows above mature deep convection using super rapid scan geostationary satellite data. *Journal of Applied Meteorology and Climatology*, 55, 1859–1887. <https://doi.org/10.1175/JAMC-D-15-0253.1>
- Bedka, K., Wang, C., Rogers, R., Carey, L. D., Feltz, W., & Kanak, J. (2015). Examining Deep Convective Cloud Evolution Using total lightning, WSR-88D, and GOES-14 super rapid scan observations within deep convective clouds. *Weather and Forecasting*, 30, 571–590. <https://doi.org/10.1175/WAF-D-14-00062.1>
- Biswas M. K., Bernardet, L., Abarca, S., Ginis, I., Grell, E., Kalina, E., et al. (2017). Hurricane Weather Research and Forecasting (HWRF) model: 2017 Scientific documentation, NCAR Technical Notes NCAR/TN-544+STR, 111 pp, DOI: <https://doi.org/10.5065/D6MK6BPR>.
- Blake, E. S., & Zelinsky, D. A. (2018). *Tropical Cyclone Report: Hurricane Harvey (AL092017)*. Miami, FL: National Hurricane Center. <https://www.nhc.noaa.gov/data/tcr/>
- Boukabara, S., Zhu, T., Tolman, H. L., Lord, S., Goodman, S., Atlas, R., & Chen, T.-C. (2016). S4: An O2R/R2O infrastructure for optimizing satellite data utilization in NOAA numerical modeling systems: A step toward bridging the gap between research and operations. *Bulletin of the American Meteorological Society*, 97, 2359–2378. <https://doi.org/10.1175/BAMS-D-14-00188.1>
- Bresky, W. C., Daniels, J. M., Bailey, A. A., & Wanzong, S. T. (2012). New methods toward minimizing the slow speed bias associated with atmospheric motion vectors. *Journal of Applied Meteorology and Climatology*, 51, 2137–2151. <https://doi.org/10.1175/JAMC-D-11-0234.1>
- Cangialosi, J. P., Latto, A. A., & Berg, R. (2018). *Tropical cyclone report: Hurricane Irma (AL112017)*. Miami, FL: National Hurricane Center. <https://www.nhc.noaa.gov/data/tcr/>
- Daniels, J., Bresky, W., Wanzong, S., & Velden, C. (2019). The GOES-R Advanced Baseline Imager (ABI) algorithm theoretical basis document for derived motion vectors, available from NOAA/NESDIS/STAR.
- Ferrier, B. S. (2005). An efficient mixed-phase cloud and precipitation scheme for use in operational NWP models. *Eos, Transactions, American Geophysical Union*, 86 (Spring Meeting Suppl.), Abstract A42A-02.
- Han, J., Wang, W., Kwon, Y. C., Hong, S., Tallapragada, V., & Yang, F. (2017). Updates in the NCEP GFS cumulus convection schemes with scale and aerosol awareness. *Weather and Forecasting*, 32, 2005–2017. <https://doi.org/10.1175/WAF-D-17-0046.1>

- Han, J., Witek, M., Teixeira, J., Sun, R., Pan, H.-L., Fletcher, J. K., & Bretherton, C. S. (2016). Implementation in the NCEP GFS of a Hybrid Eddy-Diffusivity Mass-Flux (EDMF) boundary layer parameterization with dissipative heating and modified stable boundary layer mixing. *Weather and Forecasting*, 31, 341–352. <https://doi.org/10.1175/WAF-D-15-0053.1>
- Iacono, M. J., Delamere, J. S., Mlawer, E. J., Shephard, M. W., Clough, S. A., & Collins, W. D. (2008). Radiative forcing by long-lived greenhouse gases: Calculations with the AER radiative transfer models. *Journal of Geophysical Research*, 113, D13103. <https://doi.org/10.1029/2008JD009944>
- Lim, A. H. N., Jung, J. A., & Nebuda, S. E. (2019). Tropical cyclone forecasts impact assessment from the assimilation of hourly visible, shortwave, and clear-air water vapor atmospheric motion vectors in HWRF. *Weather and Forecasting*, 34, 177–198. <https://doi.org/10.1175/WAF-D-18-0072.1>
- Lindley, T. T., Anderson, A. R., Mahale, V. N., Curl, T. S., Line, W. E., Lindstrom, S. S., & Bachmeier, A. S. (2016). Wildfire detection notifications for impact-based decision support services in Oklahoma using geostationary super rapid scan satellite imagery. *Journal of Operational Meteorology*, 4(14), 182–191. <https://doi.org/10.15191/nwajom.2016.0414>
- Line, W., Schmit, T. J., & Lindsey, D. (2016). Use of Geostationary Rapid Scan imagery by the Storm Prediction Center (SPC). *Weather and Forecasting*, 31, 483–494. <https://doi.org/10.1175/WAF-D-15-0135.1>
- Lu, J., Feng, T., Li, J., Cai, Z., Xu, X., Li, L., & Li, J. (2019). Impact of assimilating Himawari-8 derived layered precipitable water with varying cumulus and microphysics parameterization schemes on the simulation of Typhoon Hato. *Journal of Geophysical Research: Atmospheres*, 124, 3050–3071. <https://doi.org/10.1029/2018JD029364>
- Lu, X., Wang, X., Li, Y., Tong, M., & Ma, X. (2017). GSI-based ensemble-variational hybrid data assimilation for HWRF for hurricane initialization and prediction: Impact of various error covariance for airborne radar observation assimilation. *Quarterly Journal of the Royal Meteorological Society*, 143, 223–239. <https://doi.org/10.1002/qj.2914>
- Mecikalski, J. R., Jewett, C. P., Apke, J. M., & Carey, L. D. (2015). Analysis of cumulus cloud updrafts as observed with 1-min resolution super rapid scan GOES imagery. *Monthly Weather Review*, 144, 811–830. <https://doi.org/10.1175/MWR-D-14-00399.1>
- Pasch, R. J., Penny, A. B., & Berg, R. (2018). *Tropical cyclone report: Hurricane Maria (AL152017)*. Miami, FL: National Hurricane Center. <https://www.nhc.noaa.gov/data/tcr/>
- Schmit, T. J., Goodman, S. J., Gunshor, M. M., Sieglaff, J., Heidinger, A. K., Bachmeier, A. S., et al. (2014). Rapid refresh information of significant events: Preparing users for the next generation of geostationary operational satellites. *Bulletin of the American Meteorological Society*, 96(4), 561–576. <https://doi.org/10.1175/BAMS-D-13-00210.1>
- Schmit, T. J., Goodman, S. J., Lindsey, D. T., Rabin, R. M., Bedka, K. M., Gunshor, M. M., & Schmidt, C. C. (2013). Geostationary Operational Environmental Satellite (GOES)-14 super rapid scan operations to prepare for GOES-R. *Journal of Applied Remote Sensing*, 7(1), 073462. <https://doi.org/10.1117/1.JRS.7.073462>
- Schmit, T. J., Griffith, P., Gunshor, M. M., Daniels, J. M., Goodman, S. J., & Lebar, W. J. (2017). A Closer Look at the ABI on GOES-R. *Bulletin of the American Meteorological Society*, 98(4), 681–698. <https://doi.org/10.1175/BAMS-D-15-00230.1>
- Schmit, T. J., Gunshor, M. M., Menzel, W. P., Li, J., Bachmeier, S., & Gurka, J. J. (2005). Introducing the Next-generation Advanced Baseline Imager (ABI) on GOES-R. *Bulletin of the American Meteorological Society*, 86, 1079–1096. <https://doi.org/10.1175/BAMS-86-8-1079>
- Schmit, T. J., Lindstrom, S. S., Gerth, J. J., & Gunshor, M. M. (2018). Applications of the 16 Spectral Bands on the Advanced Baseline Imager (ABI). *Journal of Operational Meteorology*, 6(4), 33–46. <https://doi.org/10.15191/nwajom.2018.0604>
- Stettner, D., Velden, C., Rabin, R., Wanzong, S., Daniels, J., & Bresky, W. (2019). Development of enhanced vortex-scale atmospheric motion vectors for hurricane applications. *Remote Sensing*, 11, 1981. <https://doi.org/10.3390/rs11171981>
- Tong, M., Sippel, J., Tallapragada, V., Liu, E., Kieu, C., Kwon, I., et al. (2018). Impact of assimilating aircraft reconnaissance observations on tropical cyclone initialization and prediction using operational HWRF and GSI ensemble-variational hybrid data assimilation. *Monthly Weather Review*, 146, 4155–4177. <https://doi.org/10.1175/MWR-D-17-0380.1>
- Trahan, S., & Sparling, L. (2012). An analysis of NCEP tropical cyclones vitals and potential effects on forecasting models. *Weather and Forecasting*, 27, 744–756. <https://doi.org/10.1175/WAF-D-11-00063.1>
- Velden, C., Lewis, W. E., Bresky, W., Stettner, D., Daniels, J., & Wanzong, S. (2017). Assimilation of high-resolution satellite-derived atmospheric motion vectors: Impact on HWRF forecasts of tropical cyclone track and intensity. *Monthly Weather Review*, 145, 1107–1125. <https://doi.org/10.1175/MWR-D-16-0229.1>
- Wang, P., Li, J., Lu, B., Schmit, T. J., Lu, J., Lee, Y.-K., et al. (2018). Impact of moisture information from Advanced Himawari Imager Measurements on heavy precipitation forecasts in a regional NWP model. *Journal of Geophysical Research: Atmospheres*, 123, 6022–6038. <https://doi.org/10.1029/2017JD028012>
- Wu, T.-C., Liu, H., Majumdar, S. J., Velden, C. S., & Anderson, J. L. (2014). Influence of assimilating satellite-derived atmospheric motion vector observations on numerical analyses and forecasts of tropical cyclone track and intensity. *Monthly Weather Review*, 142, 49–71. <https://doi.org/10.1175/MWR-D-13-00023.1>
- Wu, T.-C., Velden, C. S., Majumdar, S. J., Liu, H., & Anderson, J. L. (2015). Understanding the influence of assimilating subsets of enhanced atmospheric motion vectors on numerical analyses and forecasts of tropical cyclone track and intensity with an ensemble Kalman filter. *Monthly Weather Review*, 143, 2506–2531. <https://doi.org/10.1175/MWR-D-14-00220.1>
- Zhang, S., Pu, Z., & Velden, C. S. (2018). Impact of enhanced atmospheric motion vectors on HWRF hurricane analyses and forecasts with different data assimilation configurations. *Monthly Weather Review*, 146, 1549–1569. <https://doi.org/10.1175/MWR-D-17-0136.1>